Int J Infrared Milli Waves (2006) 27: 1145–1158
DOI 10.1007/s10762-006-9096-5

ARTIFICIAL NEURAL NETWORK ANALYSIS IN INTERFEROMETRIC THz IMAGING FOR DETECTION OF LETHAL AGENTS

Aparajita Bandyopadhyay,[1] Amartya Sengupta,[1] Alexander M Sinyukov,[1]
Robert B Barat,[2] Dale E Gary,[1] Zoi-Heleni Michalopoulou[3] and John F Federici[1]

[1]*Department of Physics*
[2]*Otto York Department of Chemical Engineering*
[3]*Department of Mathematical Sciences*
New Jersey Institute of Technology, Newark, New Jersey 07102

ABSTRACT

In the context of a non-invasive, non-contact method to detect concealed lethal agents employing stand-off imaging in the Terahertz (THz) range using an interferometric detector array, the techniques of image analysis are discussed. To complement the experimental testing, extensive modeling simulates reconstructed images of lethal agents at different THz frequencies applying interferometric techniques. The composite images are consequently analyzed using artificial neural network to make positive identification of the lethal agent. This work also attempts to address issues related to the presence of barriers and isolate some suitable numerical techniques required for rapid and successful recognition of lethal agents during security screening in THz range.

Submitted to: *International Journal of Infrared and Millimeter Waves*

1. INTRODUCTION

In the wake of the acute sense of vulnerability to concealed threats, a primary focus of national security is the development of non-obtrusive, yet highly reliable schemes for monitoring and detection of different lethal agents. While several existing security screening technologies such as, X-rays, infrared, ion mobility spectrometry and others have their various advantages and disadvantages, there has been considerable interest in exploring the capabilities of Terahertz screening systems.[1]

Lying between the microwave and infrared region of the electromagnetic spectrum terahertz (THz) radiation between 0.1-10 THz (3000-30 micron in wavelength), bridges the gap between photonic and electronic devices and offers a large expanse of unused, unexplored bandwidth. Its ability to penetrate non-metallic common materials, such as clothing, plastic, ceramic, wood, and identify hidden objects, such as plastic explosives, chemicals and other materials beneath clothing and in packages[2, 3, 4, 5, 6] presents an opportunity to use THz technology in the areas of security and defense. Moreover as per present knowledge, THz radiation is harmless to living cells at the energy flux levels anticipated for security screening. The existence of spectral signatures of various explosives and chemical species in THz range increases the potential of specificity to reduce false-alarm rates. Therefore, THz technology would be able to complement and enhance existing and emerging techniques to increase operational effectiveness in security screening.[7, 8, 9]

In the present study, a novel screening method has been described in brief. It combines the spectral imaging capability of THz waves through characteristic transmission or reflection spectrum of explosive agents, with interferometric imaging techniques to provide spatial detection of such lethal agents using only a limited number of detectors. However due to the current limited availability of resources, especially suitable THz sources and detectors, the measure of the performance of the THz imager in its developmental stage cannot be estimated directly. Therefore in addition to the ongoing experimental testing of this THz imaging system,[10] extensive simulations yield spatial composite images of agents at different frequencies, thus providing spectral contrast. These images are simulated based on the spectral data obtained with a THz Time Domain Spectroscopic (THz-TDS) system and different interferometric detector configurations.

The subsequent processes of agent identification out of these composite images using artificial neural network (ANN) analysis is described in detail. Artificial neural networks are applied to the present problem of discriminating between a block of metal and a block of Composition C-4 explosive (91% RDX or cyclotrimethylenetrinitramine + 9% plasticizer) based on their spectral signatures at two different THz frequencies.[11, 12] Two distinct methodologies–Multilayer Perceptron (MLP) model and Kohonen Self Organizing Map (KSOM)–are studied in the context of identifying the agents in the reconstructed interferometric images.

2. INTERFEROMETRIC SPECTRAL IMAGING

The interferometric spectral imaging technique is suited for THz security imaging as it requires only a few individual detector elements and can image many sources of THz radiation at once. It can produce images using incoherent as well as coherent sources, and provides spectral information as well as spatial imaging data.[13, 14]

The proposed imaging interferometer consists of an array of individual detectors arranged non-periodically. As the wavefront of reflected (or transmitted) THz radiation encounters the array, each pair of detectors measures one spatial Fourier component of the incoming THz radiation as determined by the separation of the detector pair, otherwise known as a baseline. Each spatial Fourier component is represented by a point in the Fourier transform plane called the *u-v* plane. In other words, signals at two or more points in space (that is the detector aperture plane) are brought together with the proper delay and correlated both in phase and in quadrature to produce cosine and sine components (points in the Fourier transform u-v plane) of the brightness distribution. In order to determine a spatial Fourier component and hence the direction of the incoming THz wavefront, the phase delay in the arrival of the wavefront between a pair of detectors must be measured. The relative angle between the direction to the source and the baseline (an imaginary line connecting the two detectors) defines the geometric delay τ_g in arrival of the wavefront between the two detectors. All the directions that form a cone around the baseline have the same phase delay

$$\tau_g = \frac{b\sin(\alpha)}{c} \tag{1}$$

where b is the length of the baseline, c is the speed of light, and α is the relative angle. In order to determine the correct source direction, additional measurements with other orientations of the baseline must be carried out.[15]

Apart from the spatial information of different sources, the reflected wavefront also carries the characteristic spectral signature of the sources present. Therefore, by combining two or more images of the same set of objects made at two or more different THz frequencies, composite interferometric spectral images are obtained through which discrimination or classification of lethal agents, even hidden behind barriers, can be achieved using appropriate numerical techniques.

3. INTERFEROMETRIC IMAGE SIMULATIONS

In the proposed THz imager, the THz radiation incident onto the interferometric detector array corresponds to either the reflection or transmission spectrum of the objects being irradiated. Given N detectors, there are N(N-1)/2 possible pairs of baseline combinations. Thus an image of the original THz brightness distribution can be generated by evaluating the spatial Fourier components of all the different baseline pair combinations by standard Fourier inversion of the amplitude and phase information experimentally detected between detector pairs.[7] Moreover, unlike the astronomical applications where the interferometric imaging array is typically operated in the optical far field (that is, planar wavefront), for the stand-off security screening, the object to be imaged is in the near-

field region (that is, the spherical wavefront) of the imaging array. Consequently, the far-field image reconstruction must be modified to account for the wavefront curvature in the near-field. The near-field correction is calculated conceptually by repositioning the detectors from a linear arrangement to a spherical arrangement that matches the curvature of the incoming wavefront.

Figure 1 illustrates experimental interferometric image reconstruction with a linear set of detectors for a linear image in reflection mode. It explains the calculation of THz brightness distribution through measurement of THz electric field amplitudes and phases at each detector element. In order to obtain an interferometric image of an object by an N element detector array, amplitudes and phases of THz field at the point of each detector are necessary. The generated image is represented by the brightness distribution function

$$\sigma_E(\xi) = \sum_{i=1}^{N(N-1)/2} \left[\mathrm{Re}\left(C(u_i)\right)\cos\left(2\pi u_i \xi\right) - \mathrm{Im}\left(C(u_i)\right)\sin\left(2\pi u_i \xi\right) \right],$$

For detector positions x_m and x_n, $u_i = (x_n - x_m)/\lambda$ and $C(u_i) = A_i e^{i\Delta\phi_i}$ is the electric field correlation function. $A_i = E_m E_n$ and $\Delta\phi_i = \phi_m - \phi_n$ represent the product of electric field amplitudes and change in phase for each baseline pair combination, respectively.[16]

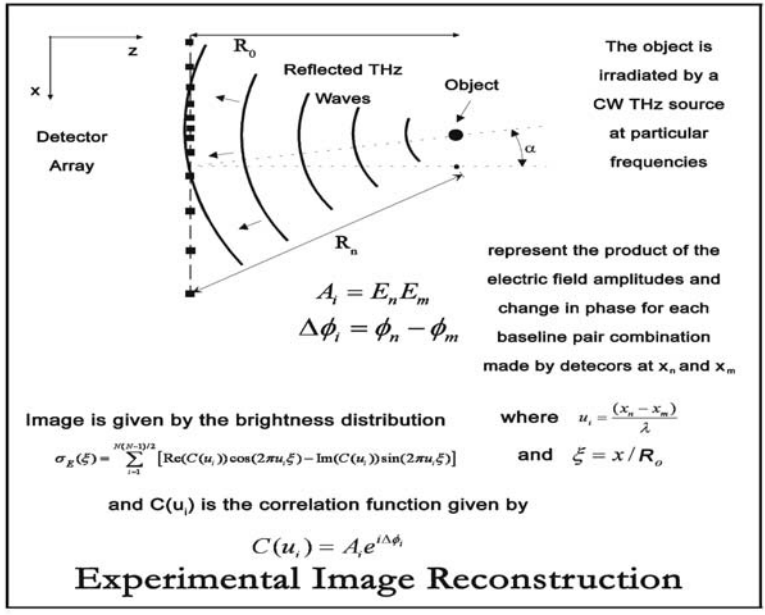

Figure 1: Flowchart showing experimental scheme for terahertz interferometric image reconstruction

As Figure 2 shows, for the interferometric image simulation, the starting point is a bitmap image of the object under study. The image is then appropriately converted to multiple images at different THz frequencies, containing the spectral characteristics of different compounds present, based on their individual THz reflection spectra. After the Fourier transform of these raw images, they are multiplied by the corresponding Fourier transform of the mask at those frequencies. These masks are the impulse response or point spread function for the imaging system. They are dependent on the specific detector configuration, and the distance between the object and detector plane. In other words, these functions are a measure of the energy spread of a central THz source. An inverse Fourier transform is applied to these products. The results are simulated reconstructed interferometric images of the object under study at those particular THz frequencies. In this study, we attempt to establish a working model for a successful spectral classification of different agents using these simulated interferometric images. Therefore linear images are sufficient as they contain all the spectroscopic information of various agents for the spectral classification purpose. However, linear images can only specify the relative positions of the agents present, but cannot describe the geometrical shapes of the same.

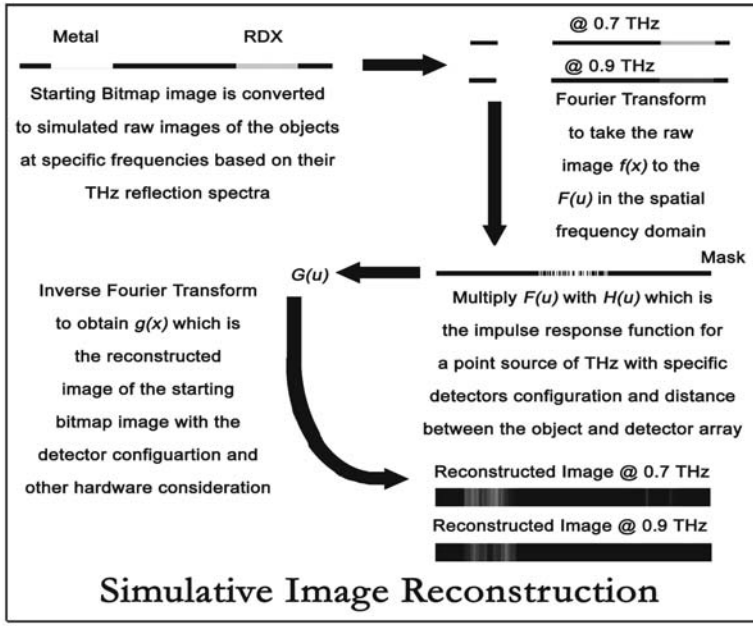

Figure 2: Flowchart showing simulation schemes for terahertz interferometric image reconstruction

4. IMAGE ANALYSIS USING ARTIFICIAL NEURAL NETWORK

Interferometric reconstructed images obtained either from experimental observation or through simulation, cannot be interpreted directly for agent identification. These images contain fringe pattern, which is characteristic artifact of the interferometric image formation, as well as additional effects due to noise, signal fluctuation and other variables. These problems make extraction of spatial and spectral information on potential hidden agents present in the images very difficult with traditional numerical approaches. Therefore, towards the realization of an efficient and accurate classification and positive identification scheme for lethal and non-lethal agents in an image, Artificial Neural Network (ANN) analysis is employed.

Inspired by biological nervous systems, ANN is essentially an evolved structure of mathematical functions that can perform a particular task of considerable complexity through supervised learning.[17] This kind of computing architecture is especially suitable for solving problems of classification, pattern recognition and identification. A network is typically trained (that is, calibrated) based on a comparison of its actual output and the desired target. Internal weighting values are adjusted until the network output matches the target description to within a minimal (acceptable) error. During training, the network produces an output to each input whereby correct outputs are reinforcing while incorrect ones cause internal adjustments in the structure of the network.[18]

The ANN is extensively used in various industrial, business and scientific applications.[19] An early application of neural networks outside the financial industry was in the area of security screening in 1989.[20] The attributes that make ANN a very suitable tool for agent identification, in contrast to the traditional statistical technique[21] or discriminant analyses,[22] are its ability to adapt to the effects of multiple variability by processing sufficiently large datasets to optimize an error criterion, and faster performance owing to its tremendous number of interconnects and simple processors.[23] There are various types of ANN architectures frequently used in the application of image processing and pattern recognition.[24] In our present study, we adopted the Multilayer Perceptron (MLP) model and the Kohonen Self-Organizing Maps (KSOM).

In the present study, we consider the problem "Metal-RDX" which is a set of images of 1 pixel by 500 pixel size as produced by the interferometric image simulation. It corresponds to an object consisting of a 2.5 cm square of gold mirror and a 2.5 cm square of Composite C 4 explosive placed 5 cm apart at a distance of 1 meter from the detector array. The detector array is linear and consists of 10 detectors. The probing frequencies are 0.7 THz and 0.9 THz, which together produce a contrast of roughly 8% for Composite C 4 in its reflection spectrum as measured with the THz Time Domain experimental set-up.[25] The interferometric image simulation and KSOM model are done using the MATLAB®.[26] The MLP model is done using the NeuroSolutions for MATLAB® software package from NeuroDimension, Inc.[27]

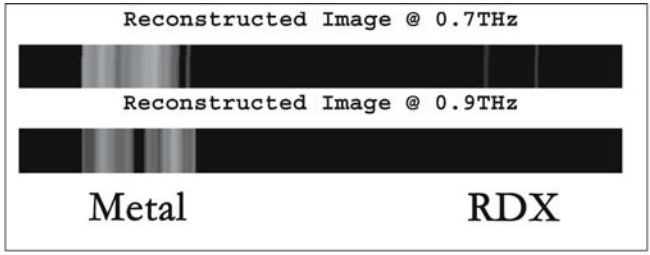

Figure 3: The reconstructed images in the Metal-RDX problem at two frequencies of interest as obtained from the simulation

Figure 3 shows the reconstructed images of the Metal-RDX object obtained through simulative image reconstruction. One may readily see the spectral contrast of the agent RDX at two THz frequencies as opposed to metal which has flat spectral response in THz range. These images are the ones that are processed by the ANNs as described in the following sections.

4a. Application of Multilayer Perceptron Model

The MLP model is the most widely used class of ANN, especially for classifications. The MLP can "learn" how to interpret large sets of input data relatively fast, though MLPs do require considerable training to be effective.[11] The MLP consists of input, hidden and output layers. The computation at the k^{th} node in a MLP considers a weighted sum (activation value net_k) of inputs (vector I_j). The output, o_k, of the node is computed by:

$$o_k = \tanh(net_k) = \tanh(\sum_{j=1}^{j} w_{kj} I_j) \quad (2)$$

where w_{kj} represent a set of weights that are optimized during the training process. Figure 4 represents a schematic of the basic structure for a MLP model. The threshold function can be varied, though *tanh* is common and effective.

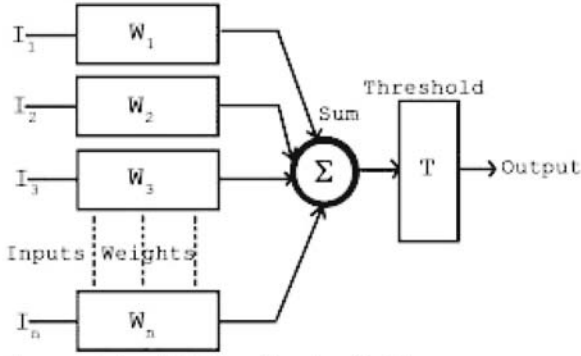

Figure 4: Schematic representation of Multilayer Perceptron Model

The reconstructed images corresponding to the object Metal-RDX are first processed to prepare the training dataset for the MLP model used in the present study. For the purpose of generating the dataset to train the MLP, the simulation produces separate images in the following manner:

i) Only a single metal square or a single RDX square is imaged at a time, keeping the size, distance, detector configuration and other factors constant.

ii) To achieve superior randomization in the training set, which essentially returns better performance of a trained ANN, the spatial position of the object is changed. In other words, the square of metal or the square of RDX is placed at different spatial locations in the image.

iii) These images are then scanned with a template of 1 pixel by 5 pixel rectangular template. Thus they are converted to input matrices where each row is assigned with a desired output of 0, 1 or 2 depending on whether the template finds background, metal or RDX during its scanning of a given row. Compared to a pixel-by-pixel approach, this method of scanning reduces the data preprocessing time considerably.

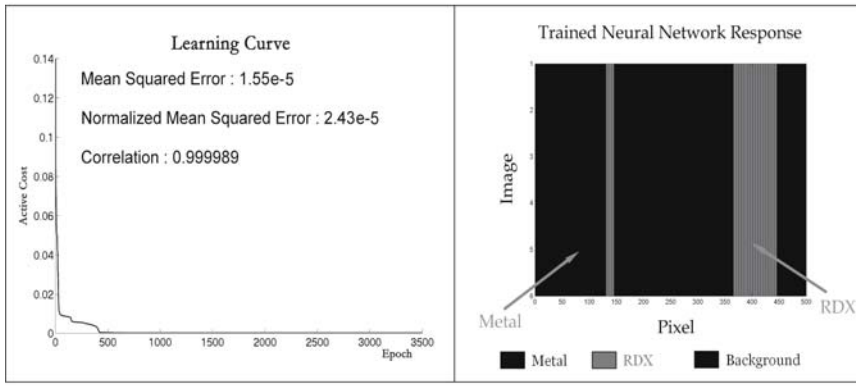

Figure 5: (left) The learning curve obtained during the training of the MLP structure used in the Metal-RDX problem with 2 hidden layers and 3500 epochs; (right) The response of the trained MLP network to the unknown input in the Metal-RDX problem

Successful training of the MLP network consisting of 2 hidden layers required less than 5000 epochs (or iterations) as illustrated by the Learning Curve of the MLP in Figure 5 (left). During this training session, the input was the set of simulated images with one agent placed on bare background at a time as described above. We opt for 2 hidden layers as we found that the active cost of the MLP with 2 hidden layers, stabilizes quickly within or less than 1000 epochs, indicating better performance. The mean square error (that is, the square of the difference between the calculated and desired output) is found to be appreciably low at 1.55E-5 with a very high correlation value, approaching 1, as

shown in the learning curve in Figure 5. This suggests a successful execution of the MLP structure in recognizing the spectral signatures of the metal and RDX. The trained MLP is then tested using another set of simulated images of individual agents on the background.

Once successfully trained and tested, the MLP network is then employed to an unknown input, that is, a set of composite images of the Metal-RDX as shown in Figure 3. The response is found to be quite satisfactory as shown in Figure 5 (right). The MLP network could recognize metal and RDX in their respective original positions. However in some of the pixel positions in between the metal and RDX squares, some ambiguities are found. This is due to the so called boundary effect where the reconstructed images themselves bear the edge effect due to the Fourier transform and subsequent finite sampling of the image space in generation of the mask. This is a fundamental problem of digital image processing.[28] When the sampling function chooses a pixel near the edge or boundary of an image, then some of the weight of the function also operates upon "invalid pixels" beyond the boundary of the real image. As a result, the intensity values which directly correspond to the spectral characteristics of the agents under concern get distorted, and therefore, the MLP cannot classify or discriminate these pixel positions accurately.

4b. Application of Kohonen Self Organizing Maps

Kohonen Self Organizing Maps are two-layer (input and output) neural networks.[29, 30] The output is typically a two-dimensional arrangement of nodes, often forming square or hexagonal maps. The number of input nodes is, in our case, equal to the number of frequencies at which we make measurements (0.7 and 0.9 THz, in the present study). Input patterns presented to the network for processing are vectors with two elements; these elements are image intensities corresponding to the same pixel at the two distinct frequencies. The number of input patterns presented to the network is the number of pixels in our images (500).

The input layer is linked to the output map through weighted connections. The weights are initially randomized, with a random mapping from input patterns to output nodes. Weights are adapted iteratively in a way that maps input patterns with a small Euclidean distance to the same or neighboring nodes. Thus, measurements corresponding to the same object are mapped to a cluster in the output space. Measurements corresponding to different objects with distinct spectral signatures will typically produce large distance and will be assigned to different clusters. The goal is to generate spatially separated clusters at the output corresponding to the distinct categories of data. The number of iterations necessary for the process to converge depends on the number of input patterns and output nodes. Convergence is here defined as the state during which the map does not change significantly between consecutive iterations. No training is required.

In this work a square output map with 25 nodes was considered; the network was presented with 500, two-element input patterns. The 5x5 output map shown in Figure 6

demonstrates that the KSOM successfully separates the three classes that are present in the data (metal, RDX, and background) into three distinct clusters; metal is mostly mapped to neighboring nodes (5,1) and (5,2), RDX is mapped to neighboring nodes (2,1), (3,1), and (2,2), and background is mapped to a large cluster of nodes with a peak at the upper left corner (1,5) of the map (a pair (x,y) denotes a KSOM node at coordinates x and y, where x and y are integers with values between 1 and 5). The intensity value at each node represents the number of elements mapped there. Higher intensity is observed in the background cluster, because the number of background pixels exceeds the numbers of metal and RDX pixels within the original interferometric image.

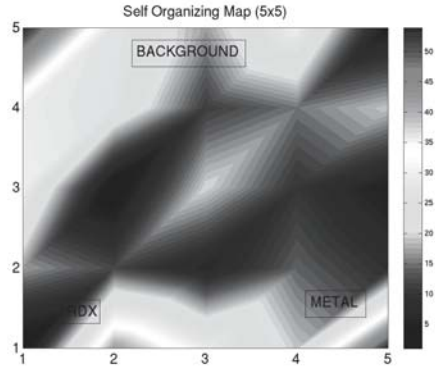

Figure 6: The response of the KSOM to the Metal-RDX problem

5. FURTHER ISSUES WITH IMAGE ANALYSIS

The fundamental approach of agent classification using ANN in THz interferometric spectral imaging as described in the above sections becomes complicated when practical issues such as the presence of barriers, nearby boundaries of different agents, comparable spectral signatures for different agent classes and other factors come into play. In this study, the impact of barriers is discussed.

In most real cases, the effects of a barrier are primarily manifested in terms of reduced signal to noise. These effects essentially lower the specificity in the classification process. A possible solution is the removal of the spectral pattern of the barrier material from the composite signature of the agent behind the barrier. It should be noted that, common barriers such as cotton, wool, leather etc. have either flat or monotonically increasing or decreasing spectral properties in the THz range. Thus it is nominally possible to "see through" the barriers and identify the agent, provided the reduction in signal to noise is not significant.

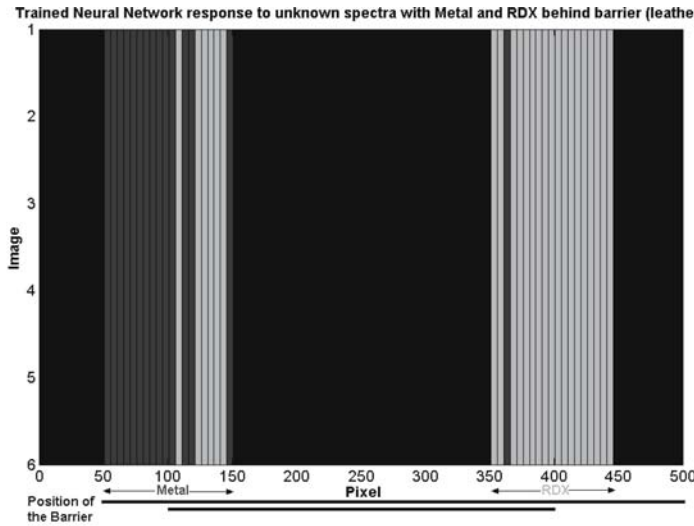

Figure 7: The response of a trained MLP network to the unknown input in the Metal-RDX problem behind leather barrier. The position of the multilayer barrier is shown at the bottom of the figure with black solid lines.

As shown in Figure 7, the Metal-RDX object was placed behind two layers of leather in the simulation. The normalized reflectance of leather are 0.34 and 0.46 at 0.7 THz and 0.9 THz respectively[31] and therefore the reduction in signal to noise due to the presence of 2 layers of leather is found to be more at 0.9 THz. The MLP network could still effectively classify the two agents and background behind the barrier. For the training of the MLP used in this case, it was found that, its performance is improved when different combinations of barrier materials such as, wool, cotton and leather were used in different spatial positions in the training dataset. One other important consideration was the fact that both the training and testing set of images have to contain some bare background. In other words, the MLP network has to "see" a portion of the background without any barrier during the training. In this case, we also observe that the effect of boundaries or the edge effect as discussed in Section 4a is enhanced due to the presence of additional boundaries of the barrier.

6. CONCLUSION

In this study, we conceived a stand-off imaging system in the Terahertz (THz) range using an interferometric detector array to detect concealed lethal agents. The composite images of simulated objects under THz illumination are analyzed using artificial neural networks to make positive identification of the lethal agent based on their spectral characteristics. We showed that a THz imager which allows sufficient signal to noise

ratio could be used to image concealed threats. The ongoing research is directed at eliminating the disadvantage of linear imaging in our current experimental set-up which does not allow the reconstruction of the geometrical shape of the target but only its position. Therefore we aim to produce stand-off two dimensional images of extended objects, especially behind barriers at a faster capturing rate experimentally and through simulation we would incorporate the statistical nature of noise and the effect of barriers in the image analysis and subsequent agent classification.

7. ACKNOWLEDGEMENT

The authors gratefully acknowledge the funding support of the Technical Support Working Group, the Department of Homeland Security, and the US Army SBIR program.

REFERENCES

[1] D. L. Woolard, E. R. Brown, M. Pepper & M. Kemp, "Terahertz Frequency Sensing and Imaging: A Time of Reckoning Future Applications?", in *Proc. IEEE*, **93**, 1722– 1743 (2005)

[2] D. J Cook, B. K. Decker, G. Maislin, & M. G. Allen, "Through container THz sensing: applications for explosives screening," in *Terahertz and Gigahertz Electronics and Photonics III*, R. J. Hwu, eds., Proc. SPIE. **5354**, 55–62 (2004)

[3] K. Kawase, Y. Ogawa & Y. Watanabe, "Non-destructive terahertz imaging of illicit drugs using spectral fingerprints," Opt. Exp. **11,** 2549–2554 (2003)

[4] D. A. Zimdars & J.S. White, "Terahertz reflection imaging for package and personnel inspection," in *Terahertz for Military and Security Applications II*, R. J. Hwu & D. L. Woolard, eds., Proc. SPIE. **5411**, 78–83 (2004)

[5] W. R. Tribe, D. A. Newnham, P. F. Taday & M. C. Kemp, "Hidden object detection: Security applications of terahertz technology," in *Terahertz and Gigahertz Electronics and Photonics III*, R. J. Hwu, ed.,*Proc. SPIE* **5354**, 44–52 (2004)

[6] Y. C. Shen, P. F. Taday & M. C. Kemp, "Terahertz spectroscopy of explosive materials," in *Passive Millimetre-Wave and Terahertz Imaging and Technology;* R. Appleby, J. M. Chamberlain, K. A. Krapels; eds. *Proc. SPIE,* **5619**, 82-89 (2004)

[7] M.C. Kemp, P. F. Taday, B. E. Cole, J. A. Cluff, A. J. Fitzgerald & W. R. Tribe, " Security applications of terahertz technology," in *Terahertz for Military and Security Applications*, R. J. Hwu & D. L. Woolard, eds., Proc. SPIE. **5070**, 44–52 (2003)

[8] M.C. Kemp, P. F. Taday, B. E. Cole, J. A. Cluff, A. J. Fitzgerald & W. R. Tribe, " Security applications of terahertz technology," in *Terahertz for Military and Security Applications*, R. J. Hwu & D. L. Woolard, eds., Proc. SPIE. **5070**, 44–52 (2003)

[9] D. M. Mittleman, M. Gupta, R. Neelamani, R.G. Baraniuk, J. V. Rudd & M. Koch, "Recent advances in terahertz imaging," Appl. Phys. B. **68**, 1085–1094 (1999)

[10] A. Bandyopadhyay, A. Stepanov, B. Schulkin, M Federici, A. Sengupta, D. Gary, J. Federici, R. Barat, Z. H. Michalopoulou & D. Zimders, "Terahertz interferometric and synthetic aperture imaging," J. Opt. Soc. Am. A (in press)

[11] K. Yamamoto, M. Yamaguchi, F. Miyamaru, M. Tani, M. Hangyo, T. Ikeda, A. Matsushita, K. Koide, M. Tatsuno, and Y. Minami, "Noninvasive inspection of C-4 explosive in mails by terahertz time-domain spectroscopy", Jpn. J. Appl. Phys. **43**, L414-L417 (2004)

[12] H. B. Liu, Y. Chen, G. J. Bastiaans, and X.-C. Zhang, "Detection and identification of explosive RDX by THz diffuse reflection spectroscopy", Opt. Express **14**, 415-423 (2006)

[13] A. R. Thompson, J. M. Moran & G. W. Swenson. Interferometry and Synthesis in Radio Astronomy, 2nd ed., Wiley Interscience, New York (2001)

[14] J. Federici, D. Gary, B. Schulkin, F. Huang, H. Altan, R. Barat & D. Zimdars, " Terahertz imaging using an interferometric array. Appl. Phys. Let., **83**, 2477-2479 (2003)

[15] K. P. Walsh, B. Schulkin, D. Gary, J. F. Federici, R. Barat & D. Zimdars, "Terahertz near-field interferometric and synthetic aperture imaging," in *Terahertz for Military and Security Applications*, R. J. Hwu & D. L. Woolard, eds., Proc. SPIE. **5411**, 9-17 (2004)

[16] A. Bandyopadhyay, A. M. Sinyukov, A. Sengupta, R. B. Barat, D. E. Gary, Z. H. Michalopoulou & J. F. Federici, "Interferometric terahertz imaging for detection of lethal agents using artificial neural network analyses," in *Proc. IEEE Sarnoff Symposium 2006* (accepted)

[17] J.C. Principe, N.R. Euliano & W.C. Lefebvre. Neural and Adaptive Systems. (John Wiley & Sons, New York, 2000)

[18] F. Kozato & G.A. Ringwood, "How slow processes can think fast in concurrent logic," in *Fast Learning and Invariant Object Recognition: The Sixth-Generation Breakthrough*, B. Soucek & the Iris Group, eds. (John Wiley & Sons, New York, 1992), pp. 47-60

[19] B. Widrow, D.E. Rumelhart & M. A. Lehr, "Neural Networks: Applications in industry, business and science," Communication of the ACM, **37**, 93-105 (1994)

[20] P.M. Shea & V. Lin, "Detection of explosives in checked airline baggage using an artificial neural system," in *Proceedings of IEEE International Joint Conference on Neural Networks* (Institute of Electrical and Electronics Engineers, New York, 1989), pp. 31-34

[21] K. Fukunaga. Introduction to Statistical Pattern Recognition (Academic Press, San Diego, 1990)

[22] G.J. McLachlan. Discriminant Analysis and Statistical Pattern Recognition (John Wiley & Sons, New York, 2004)

[23] J.E. Dayhoff. Neural Network Architectures: An Introduction (Van Norstrand Reinhold, New York, 1990)

[24] C. T. Leondes, eds. Image Processing and Pattern Recognition (Academic Press, San Diego, 1998)

[25] A. Sengupta, A. Bandyopadhyay, R.B. Barat, D.E. Gary & J.F. Federici, " THz reflection spectroscopy of Composition C 4 and its detection through interferometric imaging," in *THz and GHz Electronics and Photonics V,* R. J. Hwu ed., Proc. SPIE **6120** (In Press)

[26] The MathWorks, Inc. http://www.mathworks.com

[27] The NeuroDimension, Inc. http://www.nd.com

[28] G. J. Awcock & R. Thomas. Applied Image Processing. (McGraw-Hill Inc., New York, 1996)

[29] T. Kohonen, G. Bama, and R. Chrisley, "Statistical Pattern Recognition with Neural Networks: Benchmarking Studies," Proc. IEEE International Conference on Neural Networks,1, 1-61 (1988)

[30] J. Kangas, T. Kohonen, J. Laaksonen, O. Simula and O. Venta, "Variants of self-organizing maps," Proc. IEEE International Joint Conference on Neural Networks, **2,** 517 (1989)

[31] D. J Cook, B. K. Decker, G. Dadusc, & M. G. Allen, "Through-container THz sensing: applications for biodetection," in *Chemical and Biological Standoff Detection*, J.O. Jensen and J.M. Theriault, eds., Proc. SPIE. **5628**, 36–42 (2003)